9th AUSTRALASIAN
FLUID MECHANICS CONFERENCE,
AUCKLAND, 8-12 DECEMBER 1986

A Full Simulation of a Vortex Ring

S. K. STANAWAY[1], B. J. CANTWELL[1] and P. R. SPALART[2]

[1]Stanford University, Stanford, CA U.S.A.
[2]NASA Ames Research Center, Moffett Field, CA, U.S.A.

ABSTRACT

A three-dimensional spectral method is developed for the solution to the incompressible Navier-Stokes equations in an unbounded domain. The spectral method relies on divergence-free basis functions as proposed by Leonard (1981). The basis functions are formed using vector spherical harmonics and Jacobi polynomials together with a mapping in the radial direction.

An axisymmetric code was written and is verified using an exact solution of the Stokes equations. Preliminary results for the evolution of a vortex ring according to the Navier-Stokes equations are presented.

INTRODUCTION

The time-dependent, incompressible Navier-Stokes equations are solved in an infinite domain with disturbances near the origin which decay at infinity. In particular, the vortex ring is studied. This work is motivated on several levels.

The vortex ring is a classical flow problem which has been studied extensively as an inviscid flow. The effect of viscosity on the motion of a ring and on the interaction of two rings is not well understood quantitatively. In addition, the effect of viscosity on the stability is not known. Insights into these questions are of interest in themselves and may have useful application to inviscid "vortex methods".

The full simulation of a vortex ring is of interest in the quest to understand and model turbulence. The numerical simulation of complex, viscous flow fields is an active area of turbulence research. This type of work has been stimulated partly by the observation of organized, large-eddy motions in turbulent shear flows and also by the availability of a new generation of powerful scientific computers. Such computations can elucidate flow mechanisms that are extremely difficult or impossible to study experimentally and can provide a primary source of data for generating "empirical" turbulence models.

Vortex rings are a good candidate for such studies. They are representative of an important class of flows which are produced by a time-dependent point force (Cantwell, 1981). A delta-function forcing, for example, produces a vortex ring. The approach outlined in this paper could be extended to other members of this class, produced by more complex forcings.

Because the Reynolds number is limited by the size of the smallest scale of the flow which can be resolved, it is desirable to use a numerical approach which is highly accurate for a given number of degrees of freedom. Spectral methods are known to have exponential convergence with respect to the number of degrees of freedom. The objective, therefore, is to develop an efficient spectral method applicable to vortex ring calculations in an unbounded domain.

When applying spectral methods to differential equations, one represents the dependent variables in terms of a linear combination of known, smooth, global functions referred to as 'basis functions'. Global basis functions are appropriate for modeling incompressible flow because the propagation speed of disturbances is infinite. With such an expansion, the governing partial differential equations can be reduced to a set of ordinary differential equations for the unknown time-dependent coefficients. This is accomplished by a weighted-residual method. The truncated expansion is substituted into the partial differential equation, multiplied by chosen weight or 'test' functions, and integrated over the relevant domain. A spectral method requires, therefore, a set of basis functions and a set of test functions appropriate to a given problem.

One class of spectral methods, introduced by Leonard (1981), uses divergence-free basis functions. This has the advantage that the pressure is eliminated as an explicit variable and that the three degrees of freedom from the components of velocity are reduced to two. This approach has been applied to a circular pipe (Leonard & Wray, 1982), straight and curved channels (Moser, Moin, & Leonard, 1983) and boundary layers (Spalart, 1986). The disadvantage is that the divergence-free basis functions satisfying the boundary conditions must be found analytically, which can be difficult.

In the next section, the weighted-residual method is reviewed, and the development of the divergence-free basis functions and test functions appropriate for the present class of flows is presented. The method and code are tested using an exact solution to the axisymmetric Stokes equations. These results and preliminary studies of the evolution of an axisymmetric vortex ring are presented in the *Results* section.

DEVELOPMENT OF THE SPECTRAL METHOD

Starting with the governing equations, the weighted-residual method is illustrated. Next, the basis functions for the vortex ring are discussed and finally, they are combined with the weighted-residual method to give the spectral equations.

Weighted-Residual Method

The governing equations are momentum,

$$\mathbf{u}_t + \mathbf{u} \cdot \nabla \mathbf{u} = -\nabla p + \nu \nabla^2 \mathbf{u}, \tag{1}$$

and continuity,

$$\nabla \cdot \mathbf{u} = 0. \tag{2}$$

*Research Assistant, Department of Aeronautics and Astronautics.
†Associate Professor, Department of Aeronautics and Astronautics.
‡Research Scientist, Computational Fluid Dynamics Branch.
**Research support by NASA Ames Research Center under interchange NCA1 - IR745 - 502.

Applying the identity,

$$\mathbf{u}\cdot\nabla\mathbf{u} = \nabla(u^2/2) - \mathbf{u}\times\omega \tag{3}$$

to Eqn. (1) gives

$$\mathbf{u}_t + \nabla\Phi - \nu\nabla^2\mathbf{u} = \mathbf{u}\times\omega \quad ; \tag{4}$$

where $\Phi = p + u^2/2$. Here $\mathbf{u}$ is the velocity, ω is the vorticity, p is the kinematic pressure, and ν is the kinematic viscosity.

In a spectral method, the momentum equation is satisfied in the weighted-residual sense. This is accomplished by taking the inner product of Eqn. (4) with specified test functions, Ψ_j. The result is,

$$< \mathbf{u}_t, \Psi_j > + < \nabla\Phi, \Psi_j > - < \nu\nabla^2\mathbf{u}, \Psi_j > = < \mathbf{u}\times\omega, \Psi_j > \tag{5}$$

where $< \mathbf{a}, \mathbf{b} >$ denotes the integral of the dot product of two vectors, $\mathbf{a}$ and $\mathbf{b}$, over the volume.

Using the product rule and Green's Theorem, the second term in Eqn. (5) can be written as

$$< \nabla\Phi, \Psi_j > = \int_S \Phi(\Psi_j \cdot \mathbf{n})dS - \int_V \Phi(\nabla\cdot\Psi_j)dV. \tag{6}$$

In this form, it is clear that this term is zero when Ψ_j is defined such that $\Phi(\Psi_j\cdot\mathbf{n}) \to 0$ (fast enough) as $r\to\infty$ and $\nabla\cdot\Psi_j \equiv 0$. For the problem under study, Φ decays like $1/r^3$ as $r\to\infty$ (Cantwell, 1986). With these conditions satisfied, the pressure "drops out". The resulting equation is,

$$< \mathbf{u}_t, \Psi_j > - < \nu\nabla^2\mathbf{u}, \Psi_j > = < \mathbf{u}\times\omega, \Psi_j > \tag{7}$$

In the present approach, the test functions and basis functions will be the same.

Divergence-free basis functions

Finding an *appropriate* set of divergence-free basis functions is an art: many conditions must be satisfied. The basis functions must not only be complete for a given set of endpoint conditions and divergence-free, they should also lead to an efficient numerical method. One measure of the numerical efficiency is the sparseness of the matrices resulting from the linear terms (on the left side of Eqn. 7). Ideally, the basis functions would be orthogonal in all three spatial coordinates. In practice, this is probably impossible to achieve simply by a judicious choice of functions.

The coordinates will dictate the types of functions which are appropriate for the boundary conditions of a given problem. For the vortex ring in an unbounded domain, we chose spherical polar coordinates. An advantage of this choice is that only one direction is infinite. As described below, special care must be taken in an infinite domain. In addition, exact axisymmetric flows can be easily represented. This will be important for future studies of azimuthal instabilities. Finally, the availability of vector spherical harmonics (VSH, defined in Appendix) enables a complete, divergence-free set of basis functions to be defined analytically. Convenient differential relations of the VSH (Hill, 1953) are used to show that two of the directions provide orthogonality in the linear terms. A disadvantage of the spherical coordinate system is that in two of the three directions one cannot use Fast Fourier Transforms in transforming between real and wave-number space.

Since the vector spherical harmonics, $\mathbf{X}_{\ell m}$, $\mathbf{V}_{\ell m}$, and $\mathbf{W}_{\ell m}$, form a complete set on a sphere (Blatt & Weisskopf, 1952), an arbitrary, unsteady, three-dimensional vector field can be represented by

$$\mathbf{u}(r,\theta,\phi,t) = \sum_{\ell,m}\{F_{1_{\ell m}}(r,t)\,\mathbf{X}_{\ell m}(\theta,\phi) + F_{2_{\ell m}}(r,t)\mathbf{V}_{\ell m}(\theta,\phi) + F_{3_{\ell m}}(r,t)\,\mathbf{W}_{\ell m}(\theta,\phi)\}. \tag{8}$$

The radial functions, $F_{1_{\ell m}}$, $F_{2_{\ell m}}$, and $F_{3_{\ell m}}$, are chosen according to the constraints of a given flow, as described below. In numerical solutions, the series is truncated with $(1 \le \ell \le L)$ and $(0 \le m \le \ell)$ where the limit, L, is set according to the complexity of the flow field.

By substituting Eqn. (8) into Eqn. (2) one sees that a divergence-free field can be represented using only two functions:

$$\mathbf{u}(r,\theta,\phi,t) = \sum_{\ell,m}\left\{F^-_{\ell m}(r,t)\,\mathbf{X}_{\ell m}(\theta,\phi) + \nabla\times[F^+_{\ell m}(r,t)\,\mathbf{X}_{\ell m}(\theta,\phi)]\right\}. \tag{9}$$

The curl of $F^+_{\ell m}\mathbf{X}_{\ell m}$, defined in the Appendix, gives the expressions for $F_{2_{\ell m}}$ and $F_{3_{\ell m}}$ as a function of $F^+_{\ell m}$. This procedure amounts to using a vector potential.

Spectral Equations

In this section, the working equations are derived, with the radial functions left arbitrary.

The radial dependence and time dependence are separated by

$$F^-_{\ell m}(r,t) = \sum_{n=0}^{N} a^-_{n\ell m}(t)\, f^-_{n\ell}(r) \tag{10}$$

and

$$F^+_{\ell m}(r,t) = \sum_{n=0}^{N} a^+_{n\ell m}(t)\, f^+_{n\ell}(r)\,. \tag{11}$$

Because the test functions and the basis functions are the same, the test functions are simply

$$\Psi^- = f^-_{n'\ell'}\,\mathbf{X}_{\ell' m'}\,, \tag{12}$$

$$\text{and}\quad \Psi^+ = \nabla\times(f^+_{n'\ell'}\,\mathbf{X}_{\ell' m'}). \tag{13}$$

These expressions are combined with the velocity expansion (Eqn. 9) and substituted into the weighted-residual equation (Eqn. 7). Using orthogonality of the VSH (Eqn. 26) and the Laplacian of VSH (Eqns. 32 - 34) it can be shown that the polar and azimuthal directions are orthogonal in the time-derivative and viscous terms. As a result, for each set of wave numbers l and m, there are two sets of N ordinary differential equations with dependent variables $a^-_{n\ell m}$ and $a^+_{n\ell m}$. These working equations are,

$$A^-_{n'n}\,\frac{d\,a^-_{n\ell m}}{dt} - \nu B^-_{n'n}\,a^-_{n\ell m} = < \mathbf{u}\times\omega, f^-_{n'\ell}\,\mathbf{X}^*_{\ell m} > \tag{14}$$

$$A^+_{n'n}\,\frac{d\,a^+_{n\ell m}}{dt} - \nu B^+_{n'n}\,a^+_{n\ell m} = < \mathbf{u}\times\omega, \nabla\times(f^+_{n'\ell}\,\mathbf{X}^*_{\ell m}) > \tag{15}$$

$$\text{where}\quad A^-_{n'n} = \int_0^\infty f^-_{n\ell}\,f^-_{n'\ell}\,r^2dr\,, \tag{16}$$

$$B^-_{n'n} = \int_0^\infty L_\ell(f^-_{n\ell})f^-_{n'\ell}\,r^2dr\,, \tag{17}$$

$$A^+_{n'n} = \int_0^\infty \left[f_{2_{n\ell}}\,f_{2_{n'\ell}} + f_{3_{n\ell}}\,f_{3_{n'\ell}}\right]r^2dr\,, \tag{18}$$

$$B^+_{n'n} = \int_0^\infty \left[L_{\ell+1}(f_{2_{n\ell}})f_{2_{n'\ell}} + L_{\ell-1}(f_{3_{n\ell}})f_{3_{n'\ell}}\right]r^2dr\,, \tag{19}$$

where the operator L_ℓ is defined in the Appendix, and $\mathbf{X}^*_{\ell m}$ is the complex conjugate of $\mathbf{X}_{\ell m}$.

Radial Functions

The radial functions, $f^-_{n\ell}(r)$ and $f^+_{n\ell}(r)$, are chosen so that they

- form a complete set,
- satisfy boundary conditions,
- generate a smooth velocity field near coordinate singularities,
- satisfy parity requirements,
- and result in a numerically efficient method.

By choosing a set of polynomials which are solutions to a Sturm-Louiville problem with certain endpoint conditions, completeness is guaranteed (Gottlieb & Orzag, 1977). When vorticity is initially confined to a finite volume, the velocity decays in the far-field like $1/r^3$ and the vorticity decays exponentially (Batchelor, 1967).

For the solution to be smooth through the origin of the coordinates, certain limiting behaviors are required for each of the components ($\hat{r}$, $\hat{\theta}$, and $\hat{\phi}$) of the velocity and vorticity as $r \to 0$. These smoothness constraints are

	u^-	u^+	ω^-	ω^+
$\hat{r}$	0	$r^{\ell-1}$	$r^{\ell-1}$	0
$\hat{\theta}$	r^ℓ	$r^{\ell-1}$	$r^{\ell-1}$	r^ℓ
$\hat{\phi}$	r^ℓ	$r^{\ell-1}$	$r^{\ell-1}$	r^ℓ

This can be shown by writing a Taylor expansion in Cartesian coordinates and taking the transforms with respect to θ and ϕ. The parity requirements are governed by the spherical coordinate system. That is, $\hat{r}$ and $\hat{\phi}$ are of odd parity, and $\hat{\theta}$ is of even parity.

Numerical efficiency is more complicated to assess. Efficiency depends on the number of terms required to represent a typical solution, and on the number of operations required to advance the solution one time step.

To approximate a function in a semi-infinite domain directly, Laguerre polynomials are appropriate. This set of polynomials, however, requires many more terms to resolve a function of given complexity than Chebychev or Legendre polynomials (Gottlieb and Orzag, 1977). It is, therefore, better to map the infinite domain to a finite one and use a another set of polynomials.

The radial domain, $0 \le r \le \infty$, is mapped to the finite domain, $0 \le \xi \le 1$, by the "modified" algebraic mapping:

$$r^2 = \frac{r_1^2\, \xi g(\xi)}{1 - \xi g(\xi)} \quad \text{where} \quad g(\xi) = 1 - a\sin(\xi\pi). \tag{20}$$

The term "modified" refers to the function $g(\xi)$.

The mapping parameter, r_1, is found such that $(r_{i+1} - r_i)/r_i$ (where r_i is the ith collocation point) is a minimum at a specified radius, R (typically, R is the radius of the ring). The parameter, a, controls the degree of clustering. Therefore, a and R are chosen for a particular vorticity distribution and r_1 is then determined.

The mapping function is shown in figure 1 with clustering about $r/R = 1$ for several values of a. The collocation points, given by solid circles, are the zeros of the Jacobi polynomials of the next higher order.

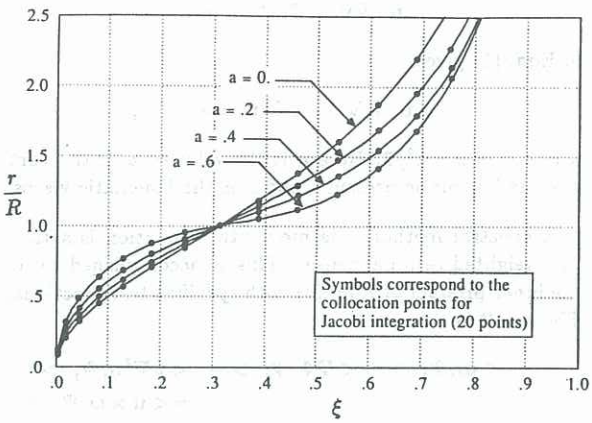

Figure 1. Modified algebraic mapping function.

This mapping, together with the radial functions,

$$f^-_{n\ell} = (1-\xi)^{3/2}\xi^{\ell/2}G_n(\xi), \tag{21}$$

$$f^+_{n\ell} = (1-\xi)\xi^{\ell/2}G_n(\xi), \tag{22}$$

satisfies the above constraints. The set of Jacobi polynomials is given by G_n, as defined in Abramowitz and Stegun (1972, p. 774) with $p = q = 1$.

With these functions, the matrices given by Eqn. 16 through Eqn. 19 are full. Trading bandwidth for a more general mapping allows the study of thinner rings.

RESULTS

The axisymmetric terms of the Navier-Stokes equations were programmed using the method described above. With the convective terms omitted, the solution is compared to an analytical solution of a Stokes vortex ring. Next, preliminary results are shown of axisymmetric rings evolving according to the Navier-Stokes equations. The starting condition is a laminar ring with Gaussian vorticity distribution through the core.

The axisymmetric form of the equations is obtained by letting $m = 0$ and no swirl is imposed by setting the ϕ component of velocity equal to 0. As a result, the $a^-_{n\ell}$ set of coefficients is zero and the two working equations (Eqns. 14 and 15) reduce to one (Eqn. 15). In the physical domain, the solution is completely specified in the $\phi = 0$ plane as shown in figure 2.

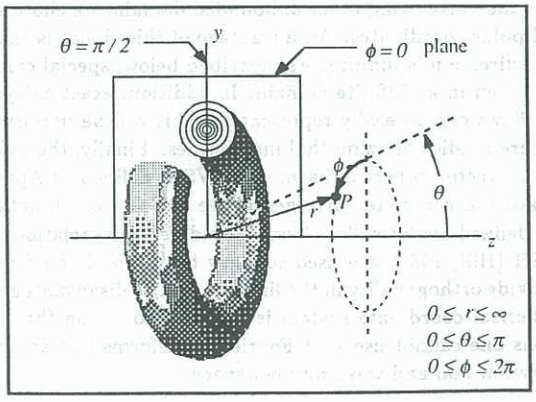

Figure 2. Vortex ring and spherical polar coordinates.

To compute the flow field, one must specify an initial velocity field or equivalently, a vorticity field. Once the initial condition is chosen, it is represented with a truncated set of basis functions. The next step is to integrate the spectral equations in time to obtain a new solution.

Because the exact solution to the Stokes vortex ring is known for all time, this is a useful test case to validate the method and much of the code. The Stokes solution for a vortex ring, derived by Allen (1984), is given by:

$$\omega(r,\theta,t) = \frac{I/\rho}{16\pi^{3/2}} \sin\theta \, r \, (\nu t)^{-5/2} \, e^{-r^2/(4\nu t)}. \qquad (23)$$

Here I is the impulse and ρ is the fluid density. The polar dependence ($\sin\theta$) is the same as that for the $\ell = 1$ basis function. As a result, the coefficients, $a^+_{n\ell}$, for $\ell \neq 1$ should be zero. This was indeed found to be the case. It is therefore sufficient to compare the computed solution to the exact solution along the radius at $\theta = \pi/2$. Figure 3 shows the Stokes solution at three times. For an expansion of 10 terms in n, and 15 collocation points, the starting condition, at $t = 1$, is so well resolved that it is indistinguishable from the exact solution. The integrated solution is then compared to the exact solution at later times, $t = 1.5$ and $t = 2$. The agreement is excellent. The mapping parameters for this case are $a = 0$ and $R = 3$.

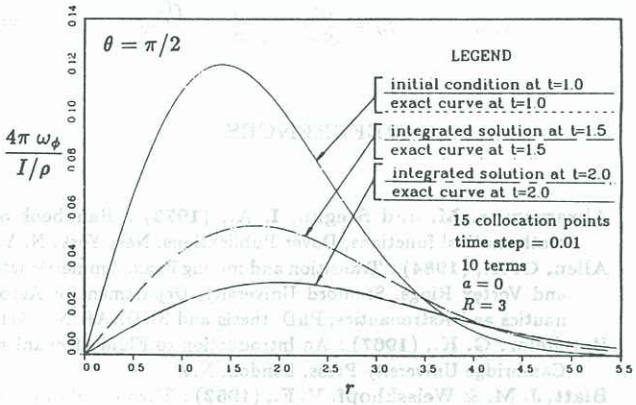

Figure 3. Radial dependence of Stokes vortex ring: comparison of the exact solution to the spectral solution.

The next case studied is a laminar vortex ring. The governing parameters are the initial Reynolds number, defined by Γ_o/ν, where Γ_o is the circulation, and ν is the kinematic viscosity, and the ratio of ring radius to core radius, r_c/R. For the cases described below, the Reynolds number is 7780, and r_c/R is 0.25, 0.35 and 0.45.

The initial vorticity distribution through the core of the ring is that of a two-dimensional viscous vortex (Batchelor, 1967) :

$$\omega = \frac{\Gamma_o}{4\pi\nu t} \, e^{-\sigma^2/(4\nu t)} \qquad (24)$$

where the radial distance, σ, is measured from the center of the core. The core radius is defined as the distance from the center of the core to the point with peak velocity.

With the vorticity distribution specified, the coefficients, $a^+_{n\ell}$ (with $N = 10$ and $L = 15$), are found, giving the approximate starting condition, shown in figure 4.

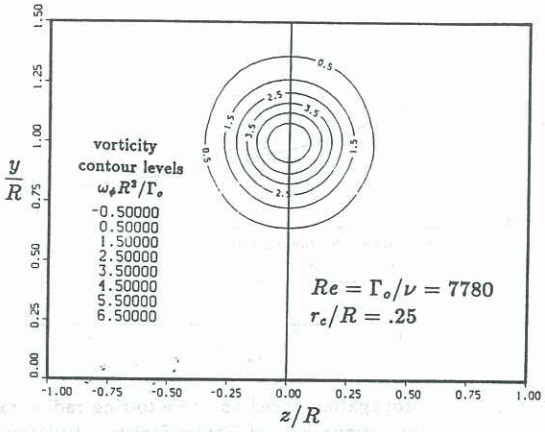

Figure 4. Axisymmetric initial condition for spectral calculations.

This initial solution is advanced in time with Eqn. (15), treating the nonlinear term pseudo-spectrally. That is, the solution is transformed from wave space to real space, the cross product performed, and the result transformed back to wave space. Explicit, Adams-Bashforth differencing is applied to the convective term, and implicit, Crank-Nicolson differencing is used for the viscous term. Both are second order accurate. The dimensionless time, $\tilde{t}$, is given by $\Gamma_o \, t/R^2$. Figure 5 shows the solution at a time, $\tilde{t}$, which is 0.526 later than the solution in figure 4 with a time step, $\Delta\tilde{t}$, of 0.0146.

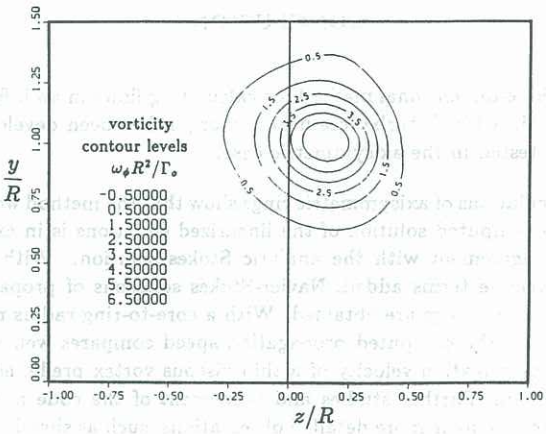

Figure 5. Navier-Stokes calculation of an evolving vortex ring.

The centroid, using the definition recommended by Saffman (1970), is at z/R equal to 0.1235. This corresponds to a propagation velocity, $\tilde{U} \equiv 4\pi RU/\Gamma_o$, of 2.95.

Saffman (1970) derived an expression for the propagation speed of a thin viscous vortex, valid for small values of r_c/R. With a Gaussian distribution of vorticity:

$$\tilde{U} = \log\left(\frac{8R}{\sqrt{4\nu t}}\right) - 0.558. \qquad (25)$$

With $r_c/R = 0.25$, Eqn. (25) gives a $\tilde{U}$ of 3.02, in good agreement with the present calculation.

Two additional cases were run with a core-to-ring radius ratio of 0.35 and 0.45. A comparison of the computed propagation speed with Saffman's thin ring propagation speed is shown in figure 6.

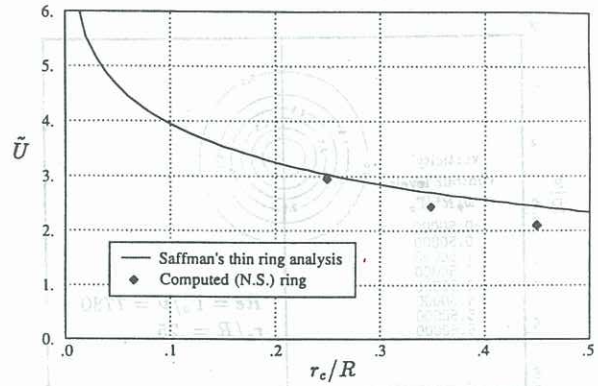

Figure 6. Propagation speed vs. core-to-ring radius ratio: comparison of Navier-Stokes calculations to thin ring theory.

The results are reasonable and the trends are as one would expect. Because of convection, the thicker rings are propagating more slowly than the thin ring analysis predicts. For larger r_c/R, the difference is greater between thin ring theory and the calculation.

The core deformation appears to be reasonable in relation to experimental observations (Maxworthy, 1972). Vorticity is beginning to be left behind the ring as though it is likely to be shed at a later time.

CONCLUSIONS

A three-dimensional method for calculating flows in an infinite domain with disturbances near the origin has been developed and tested in the axisymmetric case.

Calculations of axisymmetric rings show that the method works. The computed solution of the linearized equations is in excellent agreement with the analytic Stokes solution. With the convective terms added, Navier-Stokes solutions of propagating vortex rings are obtained. With a core-to-ring radius ratio of 0.25, the computed propagation speed compares well with the propagation velocity of a thin viscous vortex predicted by Saffman. Further studies and refinement of the code are required to make more detailed observations, such as shedding of vorticity into the wake. The observer will move with the ring, for example, so that the ring remains in the area of highest numerical resolution.

In future work, the third dimension will be included and the azimuthal instabilities of the viscous vortex ring will be studied.

APPENDIX: Vector Spherical Harmonics

$$\int_0^{2\pi}\int_0^{\pi} \mathbf{C}_{\ell m}\, \mathbf{D}^*_{\ell' m'}\, \sin\theta\, d\theta\, d\phi = \delta_{\mathrm{CD}}\, \delta_{\ell\ell'}\, \delta_{mm'} \tag{26}$$

where $\mathbf{C}$, $\mathbf{D}$ are $\mathbf{X}_{\ell m}$, $\mathbf{V}_{\ell m}$, and $\mathbf{W}_{\ell m}$.

$$\mathbf{V}_{\ell m} \equiv \hat{r}\left\{-\left(\frac{\ell+1}{2\ell+1}\right)^{1/2} Y_\ell^m\right\} + \hat{\theta}\left\{\frac{1}{[(\ell+1)(2\ell+1)]^{1/2}}\frac{\partial Y_\ell^m}{\partial\theta}\right\} + \hat{\phi}\left\{\frac{imY_\ell^m}{[(\ell+1)(2\ell+1)]^{1/2}\,\sin\theta}\right\} \tag{27}$$

$$\mathbf{X}_{\ell m} \equiv \hat{\theta}\left\{\frac{-mY_\ell^m}{[\ell(\ell+1)]^{1/2}\,\sin\theta}\right\} + \hat{\phi}\left\{\frac{-i}{[\ell(\ell+1)]^{1/2}}\frac{\partial Y_\ell^m}{\partial\theta}\right\} \tag{28}$$

$$\mathbf{W}_{\ell m} \equiv \hat{r}\left\{\left(\frac{\ell}{2\ell+1}\right)^{1/2} Y_\ell^m\right\} + \hat{\theta}\left\{\frac{1}{[\ell(2\ell+1)]^{1/2}}\frac{\partial Y_\ell^m}{\partial\theta}\right\} + \hat{\phi}\left\{\frac{imY_\ell^m}{[\ell(2\ell+1)]^{1/2}\,\sin\theta}\right\} \tag{29}$$

where Y_ℓ^m is the scalar spherical harmonic (Hill, 1953).

$$\nabla\cdot[F(r)\mathbf{X}_{\ell m}] = 0 \tag{30}$$

$$\nabla\times[F(r)\mathbf{X}_{\ell m}] = i\left(\frac{\ell}{2.\ell+1}\right)^{1/2}\left[\frac{dF}{dr}-\frac{\ell}{r}F\right]\mathbf{V}_{\ell m} + i\left(\frac{\ell+1}{2.\ell+1}\right)^{1/2}\left[\frac{dF}{dr}+\frac{\ell+1}{r}F\right]\mathbf{W}_{\ell m} \tag{31}$$

$$\nabla^2[F(r)\mathbf{V}_{\ell m}] = L_{\ell+1}(F)\mathbf{V}_{\ell m} \tag{32}$$

$$\nabla^2[F(r)\mathbf{X}_{\ell m}] = L_\ell(F)\mathbf{X}_{\ell m} \tag{33}$$

$$\nabla^2[F(r)\mathbf{W}_{\ell m}] = L_{\ell-1}(F)\mathbf{W}_{\ell m} \tag{34}$$

$$\text{and} \qquad L_\ell \equiv \frac{\partial^2}{\partial^2 r} + \frac{2}{r}\frac{\partial}{\partial r} - \frac{\ell(\ell+1)}{r^2} \tag{35}$$

REFERENCES

Abramowitz, M. and Stegun, I. A., (1972) : Handbook of mathematical functions, Dover Publications, New York, N. Y.

Allen, G. A., (1984) : Transition and mixing in axisymmetric jets and Vortex Rings, Stanford University, Department of Aeronautics and Astronautics, PhD. thesis and SUDAAR No. 541.

Batchelor, G. K., (1967) : An Introduction to Fluid Mechanics, Cambridge University Press, London, N.W.

Blatt, J. M. & Weisskhopf, V. F., (1952) : Theoretical Physics, John Wiley & Sons, New York, Appendix A & B.

Cantwell, B. J., (1981) : Organized Motion in Turbulent Flow, *Ann. Rev. Fluid Mech.* **13**, 457-515.

Cantwell, B. J., (1986) : Viscous Starting Jets. *IUTAM Symp. on Fluid Mech. in the Spirit of G. I. Taylor*, Cambridge, England. Also *J. Fluid Mech.*, (to appear).

Gottlieb, D. & Orszag, S.A., (1977) : Numerical analysis of spectral methods, NSF-CMBS Monograph 26, Soc. Ind. and Appl. Math., Philadelphia, Pa.

Hill, L. H., (1953) : The theory of vector spherical harmonics. *Am. J. Phys.* **22**, 211-214.

Leonard, A., (1981) : Divergence-free vector expansions for 3-D flow simulations. *Bull. Amer. Phys. Soc.* **26**, 1247.

Leonard, A. & Wray, A., (1982) : A new numerical method for the simulation of the three-dimensional flow in a pipe. 8th *Int. Conf. on Num. Meth. in Fluid Dyn.*, Aachen, W. Germany, June 1982. Also NASA T.M. 84267.

Maxworthy, T., (1972) : The structure and stability of vortex rings. *J. Fluid Mech.*, **51**, **1**, 15-32.

Moser, R. D. Moin, P. & Leonard, A., (1983) : A spectral numerical method for the Navier-Stokes equations with applications to Taylor-Couette flow, *J. Comp. Phys.* **52**, 524-544.

Saffman, P. G., (1970) : The velocity of viscous vortex rings. *Studies in Appl. Math.*, **XLIX**, **4**.

Spalart, P.R., (1986) : Numerical simulation of boundary layers. NASA T. M. 88220, 88221 and 88222.